

# *Packed bed electrodes. I. The electrochemical extraction of copper ions from dilute aqueous solutions*

A. K. P. CHU, M. FLEISCHMANN and G. J. HILLS

*Department of Chemistry, The University, Southampton. U.K.*

Received 1 April 1974

A study has been made of the cathodic deposition of copper ions from flowing dilute aqueous solutions onto a packed bed of graphite. The electrodeposition reaction is mass transfer controlled and expressions are presented for the cathodic current as a function of time, solution flow rate and bed characteristics. These have been verified from potentiostatic experiments. The cathode current efficiency is shown to approach 100% and packed bed electrodes are shown to be an effective means of extracting or removing metal ions from dilute solutions.

## **1. Introduction**

The electrolytic recovery of metals from dilute solutions is of considerable interest. From a conservation viewpoint, it may be noted that large quantities of dissolved metals are discarded in waste solutions and constitute an environmental hazard. From an economic view point, it may be noted that such metal is recoverable and is also susceptible to initial and direct electrochemical extraction from the dilute solutions produced by the leaching of low grade ores. However, the electrolytic removal and recovery of metal ions from dilute solutions requires the use of electrodes of high surface area and the present study is concerned with the performance of three-dimensional packed bed graphite electrodes having a large surface area per unit volume.

Several investigations of the electrochemical behaviour and performance of three-dimensional electrodes have already been reported. Fluidized bed electrodes of spherical copper particles have been employed for the electrowinning of metals [1], and a packed bed electrode consisting of porous carbon particles has been used to remove metal ions from dilute solutions [2]. Column electrodes filled with graphite particles [3, 4] and amalgamated nickel particles [5] have been used

for the electrochemical separation of metal ions, although so far, they have involved relatively small areas and low flow rates and therefore have been limited mainly to analytical applications. The present work is concerned with packed graphite beds of higher throughput and therefore of wider application.

A packed bed electrode, if sufficiently long and appropriately polarized, will therefore function as an electrochemical filter which will reduce the concentration of all electrochemical species to an acceptably low level in a single-pass of solution. Clearly such packed bed electrodes will find application in many processes of water purification in which the effluent removal of toxic components from waste streams is essential.

The structure of packed bed electrodes differs from that of conventional porous electrodes in that the flow of electrolyte in the latter is limited by the micro- and macropores of the porous matrix, whereas in the packed bed electrode, the spaces between each granule may provide additional channels through which the electrolyte can flow. This allows much higher flow rates of solution and although this structure may also reduce the bed efficiency and the bed conductivity it reduces considerably the number of dead-end pores which can seriously limit the effectiveness of the conventional

porous electrode. Perhaps more importantly, packed bed electrodes of granulate particles are very simple to prepare and use. They can easily be regenerated and repacked to restore their activity and even *in situ* the bed materials can be repacked and redistributed simply by mechanical stirring or by reversing the flow of solution.

It is evident therefore that packed bed electrodes are a suitable basis for a number of electrochemical reactor designs. However, their wide spread application requires a knowledge of their performance characteristics which has not been fully delineated. The present study is concerned to describe one aspect of performance, namely the response of a packed bed of graphite particles to cathodic electrolysis, particularly as a function of solution flow rate.

The general operational scheme for the recovery of metals using a packed graphite bed electrode is a combination of (1) the concentration cycle in which the metal is cathodically deposited onto the graphite substrate, and (2) the subsequent stripping step in which the metal is anodically redissolved into the electrolyte. This scheme resembles the anodic stripping methods which are established procedures for the analysis of traces of metals [6]. The metal concentrated on the graphite bed electrode can be anodically redissolved into a much smaller volume of electrolyte, leading to enrichment factors of  $10^3$  and beyond. The successful operation of such a metal recovery process depends on both the cathodic and anodic characteristics of the packed bed electrode; the factors determining the efficiency of the anodic cycle are discussed in the succeeding paper.

## 2. Theory

A one-dimensional model adopted for the packed bed electrode is similar to that of the porous electrode [7] and the fluidized bed electrode [8]. The solution is regarded as flowing uniformly along the axial direction (i.e. plug flow) at a steady velocity through conducting material of uniform porosity and tortuosity. The concentration of electro-reducible material will vary with the distance  $x$  from the entering surface ( $x = 0$ ) and also with the time,  $t$ , from the start of the electrolysis. For the copper deposition reaction studied here the cathodic process is fast, i.e. mass transfer

controlled, and the limiting diffusion-controlled current  $dI$  at a plane in the bed can be expressed in terms of the concentration in a thin disc at that plane and the diffusion layer thickness,  $\delta$ , determined by the flow rate, i.e.

$$dI(x, t) = \frac{nFaADc(x, t)dx}{\delta}, \quad (1)$$

where  $a$  is the cross sectional area of the bed,  $A$  is the specific area of the bed material in  $\text{cm}^2$  per  $\text{cm}^3$  and  $dx$  is the infinitesimal thickness of the disc. The other terms have their usual significance. The total current  $I$  is therefore obtained by integrating this expression over the length of the bed  $L$ , i.e.

$$I(t) = \frac{nFAD}{\delta} \int_0^L c(x, t) dx. \quad (2)$$

We consider a solution of initial concentration  $c_0$  flowing through the bed with a uniform exit velocity  $u$ . If the porosity or voidage of the bed is  $\epsilon$ , the geometric volume concentration will be  $\epsilon c$  and the actual solution velocity  $u/\epsilon$ . In terms of these quantities, the concentration  $c(x, t)$  may be formulated by taking a material balance over a differential element of the bed. For the liquid phase,

$$\epsilon \frac{\partial c}{\partial t} = -u \frac{\partial c}{\partial x} - \epsilon k_c A c + k_a A \theta, \quad (3)$$

where  $k_c$  and  $k_a$  are the electrochemical rate constants for the cathodic and anodic reactions [9].

The corresponding material balance for the solid, graphite phase is

$$\Omega \frac{\partial \theta}{\partial t} = \epsilon k_c A c - k_a A \theta, \quad (4)$$

where  $\theta$  is the fractional coverage of the graphite surface by deposited metal and  $\Omega$  is the saturation coverage. In the present work, the overpotential is sufficiently large and negative for the rate of the reverse, dissolution reaction to be negligible, i.e.  $k_a \theta \ll k_c c$ , in which case the material balance of the solid phase has a negligible effect on the cathodic process.

For a diffusion controlled electrodeposition,  $k_c$  is no longer a function of overpotential and can be expressed as

$$k_c = k_m = \frac{D}{\delta}, \quad (5)$$

where  $k_m$  is the mass transfer coefficient. Under these simplifying conditions, Equations 3 and 4 become

$$\frac{\partial c}{\partial t} = -\frac{u}{\epsilon} \left( \frac{\partial c}{\partial x} \right) - \frac{DAc}{\delta} \quad (6)$$

and

$$\frac{\partial \theta}{\partial t} = \frac{\epsilon DA c}{\Omega \delta} \quad (7)$$

Equation 6 can be solved by the method of Laplace transforms in terms of the following boundary condition:

$$c = c_0 \epsilon : 0 < x < L, t = 0 \quad (8)$$

The appropriate transform is

$$\bar{c} = \frac{c_0 \epsilon}{[S + (DA/\delta)]} + \frac{c_0 (\epsilon DA/\delta)}{S[S + (DA/\delta)]} \exp\left(-\frac{DA \epsilon x}{\delta u}\right) \exp\left(-\frac{\epsilon S x}{u}\right) \quad (9)$$

and the inverse transform leads to two solutions, depending on the time domain.

(i) For  $t > \epsilon x/u$ , the solution is

$$c(x, t) = c_0 \epsilon \times \left[ \exp\left(-\frac{DA t}{\delta}\right) + \left(1 - \exp\left(-\frac{DA t}{\delta}\right)\right) \exp\left(-\frac{x}{\lambda}\right) \right] \quad (10)$$

where  $\lambda$  is the characteristic length [8] given by

$$\lambda = \frac{\delta u}{DA \epsilon} \quad (11)$$

For an electrode of length  $L$ , the total cell current is obtained by substituting Equation 10 into Equation 2 and integrating over the length of the electrode i.e.

$$I(t) = n F a c_0 \times \left[ \frac{AD \epsilon L}{\delta} \exp\left(-\frac{DA t}{\delta}\right) + u \left(1 - \exp\left(-\frac{L}{\lambda}\right)\right) \left(1 - \exp\left(-\frac{DA t}{\delta}\right)\right) \right] \quad (12)$$

(ii) For  $t < \epsilon x/u$ , the solution is

$$c(t) = c_0 \epsilon \exp\left(-\frac{DA t}{\delta}\right) \quad (13)$$

and the corresponding total current is

$$I(t) = \frac{n F a A c_0 D \epsilon L}{\delta} \exp\left(-\frac{DA t}{\delta}\right) \quad (14)$$

### 3. Experimental

#### 3.1. Cell construction and packing materials

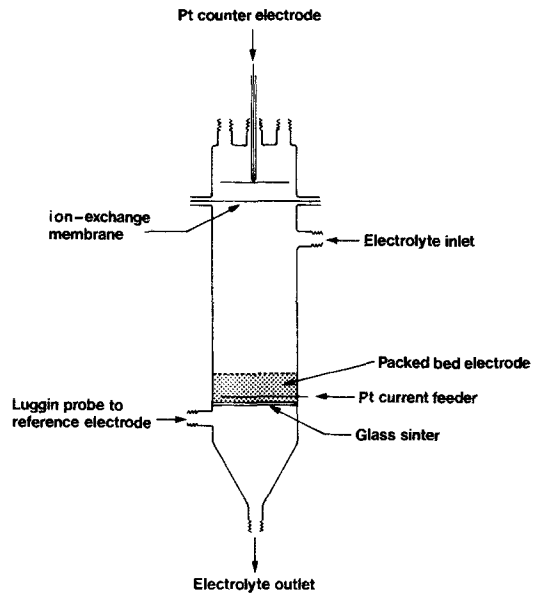


Fig. 1. Packed bed cell.

The packed bed electrode shown in Fig. 1 is similar in design to the fluidized bed electrode [1] except that the solution is made to flow downwards and thereby to consolidate the bed. The packed bed material was prepared by grinding porous, granular graphite (Elektrographite) and collecting the sieved fraction of 0.8 – 1 mm diameter particles and by washing it with nitric acid and distilled water.

These graphite particles were supported on a sintered glass disc (3.4 cm diameter) and packed to an initial, dry height of 1 to 2.2 cm. A platinum spiral seated on the sintered glass disc was used as the current feeder to the packed bed electrode. The counter electrode consisted of a platinum spiral separated from the packed bed electrode by an ion-exchange membrane (Permaplex A-20). A saturated calomel electrode was used as the reference electrode.

### 3.2 Solution and circulation

The study of bed performance was made on dilute copper sulphate solutions, i.e. approximately  $10^{-4}$  M solutions of cupric sulphate in either 1 M sulphuric acid or 1 M  $\text{Na}_2\text{SO}_4 + 10^{-3}$  M  $\text{H}_2\text{SO}_4$ . The concentrations of  $\text{CuSO}_4$  during and after electro-deposition were determined by atomic absorption spectroscopy. Approximately 2 l of solution were circulated using an impeller pump. The rate of flow was controlled by a needle valve and measured with a flow meter. Flow rates of 50 to 800  $\text{cm}^3 \text{min}^{-1}$  were used although it was evident that much higher flow rates could be tolerated.

It was necessary to remove dissolved oxygen which would otherwise give rise to a large background current. First, nitrogen was bubbled through the solution of supporting electrolyte, in this case 1 M  $\text{H}_2\text{SO}_4$ , contained in the reservoir and this solution was then pre-electrolyzed using the bed as a cathode to remove the remaining traces of oxygen. When the residual reduction current had fallen to  $< 2$  mA, the pre-electrolysis was terminated and sufficient oxygen-free concentrated copper sulphate solution was injected to give a final concentration of  $10^{-4}$  M. After further circulation the deposition process was begun.

### 3.3 Instrumentation

For the potential step measurements, the circuit consisted of a potentiostat (Chemical Electronics, Model TR-40/3A) programmed with a wave form generator (Chemical Electronics, Model RB1S). The current flowing through the packed bed cell was measured as the potential across a standard resistor and outputted to an X-Y recorder (Hewlett Packard, Model 7040A) and to an electronic integrator. For the faster potentiostatic studies, the output signal in the form of a current-time transient was first stored in a signal averager (Hi-Tek Instruments Model A1) and then displayed on an X-Y recorder.

### 3.4 Cathodic deposition cycle

The copper ions to be removed from the dilute solution were extracted or concentrated by electro-deposition onto the graphite substrate of the bed. The deposition processes were carried out

potentiostatically, the potential of the electrode being stepped from an anodic rest potential to  $-0.4$  V versus S.C.E. This potential, which corresponds to the limiting current region for the electro-deposition of copper, was held constant for a fixed period, defined here as the concentration time,  $\tau$ .

Two sequences were used for the extraction or concentration of copper: (1) *single-pass* where the solution was passed through the packed cell only once and (2) *multiple-pass* where the solution was continuously recirculated from the reservoir. In the single-pass sequence, the inlet concentration of cupric sulphate was constant, whereas in the case of multiple-pass, the inlet concentration decreased with the time of electrolysis.

## 4. Results and discussion

### 4.1. Polarization curves

Fig. 2 shows the current-potential behaviour for copper deposition from  $0.8 \times 10^{-4}$  M  $\text{CuSO}_4$  onto a 1.2 cm bed at a flow rate ranging from 50 to 600  $\text{cm}^3 \text{min}^{-1}$ . At each steady flow rate, well defined limiting currents were observed which increased with the flow rate as expected. Evidently, within the corresponding range of potential, the copper deposition process is mass transfer controlled throughout the bed.

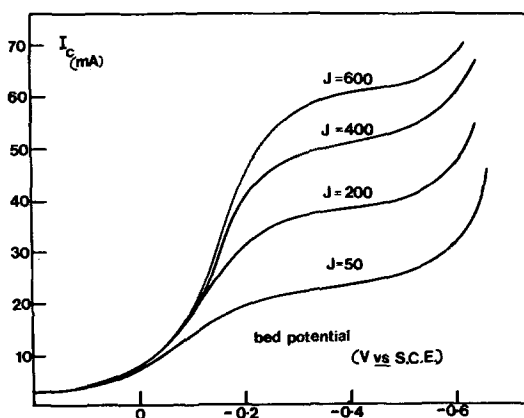


Fig. 2. Polarization curves at various flow rates for the electro-deposition of copper from  $0.8 \times 10^{-4}$  M  $\text{CuSO}_4$  onto a 1.2 cm bed. The graphite bed potential was swept linearly at  $3 \text{ mV s}^{-1}$  from  $+0.2$  to  $-0.7$  V (versus S.C.E.)

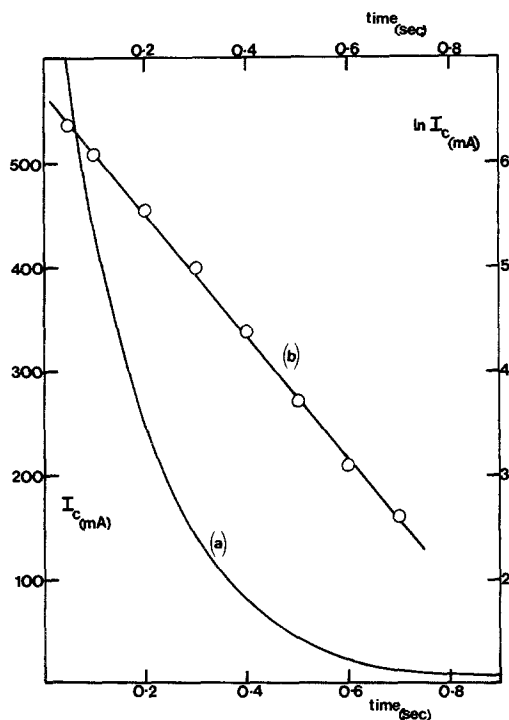


Fig. 3. Current-time transients for the potentiostatic electro-deposition of copper from  $0.8 \times 10^{-4} M$   $\text{CuSO}_4$  onto a 1.2 cm bed (cathode potential =  $-0.4$  V versus S.C.E.; solution flow rate =  $400 \text{ cm}^3 \text{ min}^{-1}$ ; base potential =  $-0.1$  V).

#### 4.2 Potentiostatic transients

For a short time domain such that  $t < \epsilon L/u$ , the current time transient may be described by Equation 14 which predicts an exponential relationship for the decrease of the current with time. For example, taking  $\epsilon = 0.5$ ,  $L = 1.2$  cm and  $u = 0.66 \text{ cm s}^{-1}$ , Equation 14 should be valid for  $t < 0.9$  s. A potentiostatic transient measured in this time domain is shown in Fig. 3 (as curve *a*) which confirms the exponential form as does the linear plot of  $\ln I$  versus  $t$  (Fig. 3, line *b*). From the intercept or the slope of this plot, the mass transfer coefficient  $k_m = D/\delta$  may be determined, provided that  $\epsilon$  and  $A$  are known.

For longer times such that  $t > \epsilon L/u$ , the  $I-t$  relationship is that of Equation 12 which can be rearranged to

$$I(t) = I_\infty + \left[ \frac{nFaAc_0DL\epsilon}{\delta} - I_\infty \right] \exp\left(-\frac{DA t}{\delta}\right), \quad (15)$$

where  $I_\infty$  is the steady state current given below, i.e. by Equation 16. According to Equation 15, a plot of  $\ln [I(t) - I_\infty]$  versus  $t$  should give a straight line but the transients in the present work were too short for this to be verified.

#### 4.3. Single-pass

The steady state electrodeposition current for a single-pass may be obtained from Equation 12 by setting  $t$  to a large value. The steady state current  $I_\infty$  so obtained is of the form [8]

$$I_\infty = nFauc_0 \left[ 1 - \exp\left(-\frac{L}{\lambda}\right) \right], \quad (16)$$

where  $\lambda$  is defined by Equation 11.

If the length of the packed bed electrode approaches infinity, the current is linearly related to  $u$  and is the maximum current for the particular configuration and flow rate [8]. However, if the length of the electrode is small, as under the present experimental conditions, the relation of  $I_\infty$  to  $u$  is not linear because of the exponential term.

Fig. 4 shows the single-pass steady state current at various flow rates for bed length of 2.2 cm.

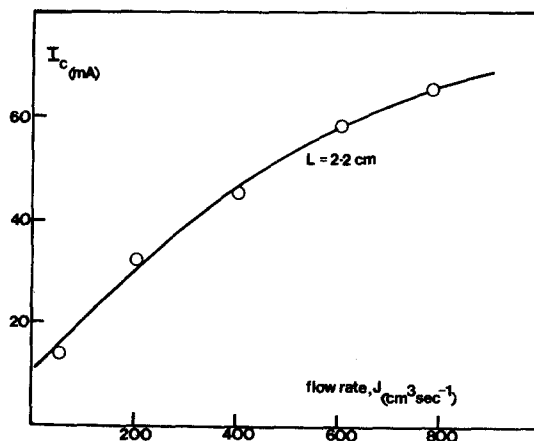


Fig. 4. Steady state cathodic current as a function of flow rate of  $10^{-4} M$   $\text{CuSO}_4$ .

The steady state emergent concentration,  $c_L$ , i.e. the concentration of the electro-active species leaving the packed bed cell, for a single-pass concentration process is obtained from Equation 10 as

$$c_L = c_0 \exp\left(-\frac{L}{\lambda}\right) = c_0 \exp\left(-\frac{\epsilon DAL}{\delta u}\right), \quad (17)$$

i.e.  $c_L$  is proportional to the product of  $\delta$  and  $u$ , inversely proportional to  $L$  and can be calculated from a knowledge of  $\lambda$  (see below and especially Table 2).

The efficiency of extracting metal ions from dilute solution by a single-pass deposition process may be defined as

$$\frac{c_0 - c_L}{c_0} = 1 - \exp\left(-\frac{L}{\lambda}\right). \quad (18)$$

Theoretically, therefore, the removing, stripping or extraction efficiency only reaches 100% when  $L$  approaches infinity or when  $u$  approaches zero. However, acceptably high efficiencies can be obtained using finite values of  $u$  and  $L$  as is shown in Table 1.

Table 1. Calculated extraction efficiencies for flow rate and bed lengths

flow rate $\text{cm}^3 \text{min}^{-1}$	$\lambda$ (from Table 2)	Bed Length (cm)						
		1.2	2.2	5	10	20	25	30
50	1.2	63	84	98	100	100	100	100
200	3.2	31	50	89	96	99.2	100	100
400	5.1	21	35	62	86	98	99.3	99.7
600	6.3	17	30	55	80	96	98	99.1
780	7.3	15	26	50	75	94	97	98

Fig. 5 shows the effect of flow rate on the extraction efficiency, the outflow concentrations  $c_L$  at various flow rates being determined by atomic absorption spectroscopy. The extraction efficiency is seen to increase with the decrease in flow rate and to approach 100% at low flow rates. The corresponding theoretical extraction efficiencies calculated by Equation 18 using experimental values of  $\lambda$  are shown in Fig. 5 as the continuous lines and it may be concluded that there is reasonable agreement between theory and practice. (The values of  $\lambda$  are given below in Table 2).

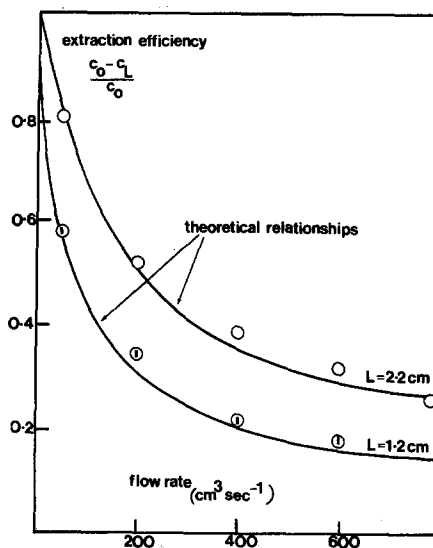


Fig. 5. Extraction efficiency as a function of the flow rate of  $10^{-4}$  M  $\text{CuSO}_4$ .

#### 4.4. Multiple-pass

The electrodeposition of copper ions onto a packed bed electrode from dilute solution can also be carried out in a multiple-pass process in which a fixed volume of solution is circulated continuously through the bed. Under these conditions, the cathodic current decreases with time as the concentration of copper ions falls. If the packed bed electrode is connected to a reservoir containing solution of volume  $V$ , the concentration of copper ions decreases with the time of electrolysis according to the relationship

$$V \frac{dc_0}{dt} = auc_L - auc_0, \quad (19)$$

where  $c_L$  is the concentration of the electro-active species leaving the packed bed cell. Equation 19 can be integrated using the value of  $c_L$  from Equation 17 to give

$$c_0 = c_0^0 \exp\left[-\frac{aut}{V} (1 - \exp(L/\lambda))\right], \quad (20)$$

where  $c_0^0$  is initial inlet concentration of the electro-active species.

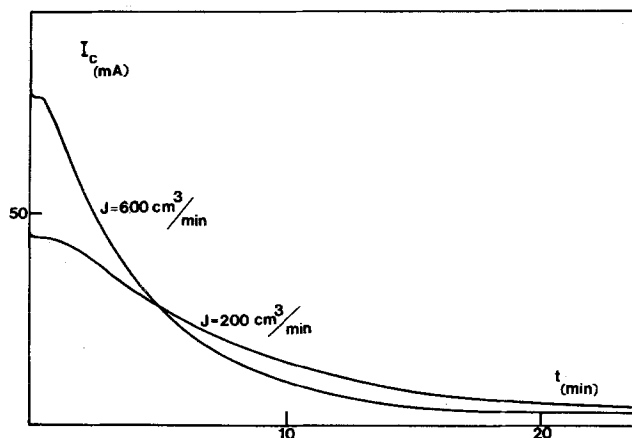
The deposition current as a function of time is then obtained by combining Equations 20 and 16, i.e.

Table 2. Derived values of  $\lambda$  for a range of flow rates

Flow rate $\text{cm}^3 \text{min}^{-1}$	Single-pass*		Multiple-pass†		Mean values
	$L = 1.2 \text{ cm}$	$L = 2.2 \text{ cm}$	$L = 1.2 \text{ cm}$	$L = 2.2 \text{ cm}$	
50	1.36	1.09	—	—	1.2
200	3.21	3.21	3.20	3.15	3.2
400	5.02	5.12	4.83	5.37	5.1
600	6.06	6.20	6.52	6.54	6.3
780	7.45	7.36	7.06	7.13	7.3

\* determined by applying Equation 16

† determined by applying Equation 21

Fig. 6. Long term current-time profiles for the extraction of copper onto a 2.2 cm bed from 950  $\text{cm}^3$  of  $1.3 \times 10^{-4} \text{ M}$   $\text{CuSO}_4$  in 1 M  $\text{H}_2\text{SO}_4$  continuously circulated from a reservoir.

$$I = nFauc_0^0 (1 - \exp(-L/\lambda) [\exp(-au/V[1 - \exp(L/\lambda)]t)]) \quad (21)$$

Equation 21 predicts that the current decreases exponentially with time, as is observed in Fig. 6 which shows a typical current-time profile of a multiple-pass extraction process. For a solution flow rate of  $600 \text{ cm}^3 \text{ min}^{-1}$ , the deposition current reached the background current after 20 min of electrolysis and the concentration of copper determined by atomic adsorption spectroscopy was  $2.4 \times 10^{-6} \text{ M}$  corresponding to an extraction efficiency of 98%. The concentration of copper after 12 min of electrolysis, i.e. at the approach to the background current was  $8 \times 10^{-6} \text{ M}$  corresponding to 94% extraction efficiency. Since the cathodic current efficiency decreases progress-

ively as the contribution of the background current to the total current increases, there will be, from an economic viewpoint, an optimal electrolysis time and therefore an optimal final concentration.

The characteristic length  $\lambda$  defined by Equation 11 can be calculated from the intercept of the plot  $\ln I$  versus  $t$ , according to Equation 21 and from the single-pass steady state current according to Equation 17. The values of  $\lambda$  for various flow rates are shown in Table 2 which indicates that  $\lambda$  increases with increasing flow rate. Once the value of  $\lambda$  is known, Equations 16 and 17 can be applied to the design of electrochemical reactors.

#### Acknowledgement.

The authors thank N.E.R.C. for general support and for a Fellowship to one of us (A.K.P.C.)

---

**References**

- [1] M. Fleischmann, J. W. Oldfield and L. Tennakoon, *J. App. Electrochem.*, **1** (1971) 103.
- [2] D. N. Bennion and J. Newman, *ibid.* **2** (1972) 113.
- [3] W. J. Blaedel and J. H. Strohl, *Anal. Chem.*, **36** (1964) 1245.
- [4] D. K. Roe, *Anal. Chem.* **36** (1964) 2371.
- [5] S. Kihara, *J. Electroanal. Chem.*, **45** (1973) 31.
- [6] E. Bardrecht, 'Electroanalytical Chemistry', Vol. 2, pp. 53-109 Ed. A. J. Bard, Marcel Dekker, New York, (1967).
- [7] J. Newman and C. W. Tobias, *J. Electrochem. Soc.*, **109** (1962) 1183.
- [8] M. Fleischmann and J. W. Oldfield, *J. Electroanal. Chem.*, **29** (1971) 211.
- [9] P. Delehay, 'New Instrumental Methods in Electrochemistry', p. 34 Interscience Publishers, Inc., New York, (1954).